Remote Sensing Letters

ISSN: 2150-704X (Print) 2150-7058 (Online) Journal homepage: http://www.tandfonline.com/loi/trsl20

A fully data-driven method for predicting Antarctic sea ice concentrations using temporal mixture analysis and an autoregressive model

Junhwa Chi & Hyun-Cheol Kim

To cite this article: Junhwa Chi & Hyun-Cheol Kim (2017) A fully data-driven method for predicting Antarctic sea ice concentrations using temporal mixture analysis and an autoregressive model, Remote Sensing Letters, 8:2, 106-115, DOI: 10.1080/2150704X.2016.1234726

To link to this article: http://dx.doi.org/10.1080/2150704X.2016.1234726

REMOTE SENSING LETTERS, 2017
VOL. 8, NO. 2, 106–115
http://dx.doi.org/10.1080/2150704X.2016.1234726

Taylor & Francis
Taylor & Francis Group

A fully data-driven method for predicting Antarctic sea ice concentrations using temporal mixture analysis and an autoregressive model

Junhwa Chi and Hyun-Cheol Kim

Korea Polar Research Institute, Unit of Arctic Sea-Ice Prediction, Incheon, Korea

ABSTRACT

While sea ice dynamics have been gaining increased attention in climate change and global warming studies, remote sensing (RS) sensors, capable of detecting and characterizing detailed information on targets of interest, have come to play a critical role in acquiring image data over extended and inaccessible areas. Passive microwave sensors have been the most effective and consistent tool for characterizing daily sea ice cover at global scale. However, it is typically challenging to study temporally successive data acquired at high time frequencies, referred to as hypertemporal data. To address this issue, among various RS analysis techniques, temporal mixture analysis (TMA) approaches are often investigated for characterizing seasonal characteristics of environmental factors including sea ice concentration (SIC) in this study. The goal of the present study is to predict daily Antarctic SICs for 1 year through a combination of TMA results and time series analysis (TSA) without incorporation of environmental factors. First, temporally most significant sea ice signals, referred to as temporal endmembers (EMs), were found using signal processing algorithms, and then corresponding fractional abundances (FAs) associated with each EM were calculated using least squares solution. Using these FAs, subsequently, a single autoregressive (AR) model that typically fits all Antarctic SIC data for the period 1979–2013 was applied to predict SIC values for 2014. Daily SIC data reconstructed using the proposed method were qualitatively and quantitatively compared to those of using real FAs derived from a spectral unmixing method. It was found that AR model trained by the proposed method successfully predicts new FAs for 2014 and the FAs should be used to reconstruct resulting 2014 daily SIC images.

ARTICLE HISTORY
Received 27 April 2016
Accepted 5 September 2016

1. Introduction

Revealing high latitude temperature trends has been receiving more and more attention in climate change and global warming research community. Sea ice in the Northern Hemisphere has exhibited a long-term diminishing trend, and the maximum sea ice extent in 2015 was the lowest on record, whereas sea ice in the Southern Hemisphere has been expanding for decades, even though average Antarctic surface temperatures

CONTACT Junhwa Chi jhchi@kopri.re.kr Korea Polar Research Institute, Unit of Arctic Sea-Ice Prediction, Incheon, Korea.

were close to the highest temperatures observed (Screen 2011). Unlike the Arctic, the Antarctic is a large continent surrounded by an ocean. Due to this geological condition, sea ice has more room to expand in the winter and exhibits great spatial variability. Specifically, sea ice of the Ross Sea has significantly increased, while in the Amundsen Sea it has exhibited a negative trend (Screen 2011).

Recent advances in remote sensing (RS), motivated by a desire to detect and characterize detailed information on targets of interest over extended areas, have led to the development of advanced sensors and have facilitated investigations of various research topics. While most RS applications are designed to obtain meaningful information from images acquired at specific time, in some applications that are related to time, univariate information (e.g., the normalized difference vegetation index (NDVI), sea ice concentration (SIC), etc.) acquired at multiple temporal instances has revealed temporal characteristics of targets (Piwowar, Peddle, and Ledrew 1998; Chi, Kim, and Kang 2016). SIC is typically estimated using passive microwave data because of the daily revisit cycle, the relatively low sensitivity to atmospheric water content and clouds, and the large contrast in emissivity between open water and sea ice (Comiso et al. 1997; Ivanova et al. 2014). Temporal mixture analysis (TMA) is an extension of the spectral mixture analysis (SMA), also known as *spectral unmixing*, of optical RS data. Increasing attention and discussions about TMA among the various analysis techniques designed to exploit time series (TS) data has recently been raised for use in characterizing long-term TS. Unlike SMA, which is used to estimate physical amounts of pure spectral components in a single RS image, TMA provides seasonal characteristics of univariate information, such as SIC, and a unique summary of long-term TS (Piwowar, Peddle, and Ledrew 1998; Chi, Kim, and Kang 2016). In addition to sea ice studies, TMA has been applied to various applications. Li and Wu (2014) developed phenology-based TMA methods to quantify fractional abundances (FAs) of impervious surface area using multi-temporal moderate resolution imaging spectroradiometer NDVI. Li and Wu (2015) proposed an automatic endmember (EM) selection method for TMA that incorporates land use and land cover probability information derived from socio-economic and environmental drivers. All of the studies reviewed here support TMA as a promising method for characterizing the seasonality of ground targets.

A recent study conducted by Chi, Kim, and Kang (2016) characterized Antarctic daily SICs on a long-term basis using machine-learning-based TMA method without incorporating prior knowledge of seasonal sea. Temporally representative EMs were identified from 36 years of daily SIC data and were then used to estimate corresponding FAs of each temporal EM. In this article, a new means of predicting daily SIC for the present year (2014) using TMA results (i.e., FAs) derived from previous years (1979–2013) reported in Chi, Kim, and Kang (2016) and using TSA is proposed. Since the proposed approach is a fully data-driven method without incorporating any environmental factors to predict SICs, the predicted SICs do not contain or minimize the impact of anomalous SIC values.

2. Methodology

TMA can be applied to temporal RS data generated by any univariate information according to time order. In the present study, we examine 36 years of daily Antarctic SIC data acquired from 1979 to 2014, provided by the National Snow and Ice Data Center (NSIDC), based on the assumption that the data quality is promised at a global

scale. The National Aeronautics and Space Administration team algorithm to generate consistent SICs from different sensors was applied to passive microwave sensors at a 25 km spatial resolution in the polar stereographic projection (Cavalieri et al. 1996).

2.1. *TMA*

Unlike SMA, very limited research has been conducted on TMA, as it is difficult to acquire high time frequency RS data. TMA stemming from SMA is generally built with two stages to handle the temporal mixing problems based on the 'linearity assumption' of mixing models: (1) finding temporally unique signatures of pure or extreme signatures, referred to as temporal EMs, using a machine-learning approach as a quantitative and automated identification and (2) decomposing each temporally mixed pixel in the TS images into a collection of temporal EMs at subpixel levels, using linear mixing models (Keshava and Mustard 2002).

Instead of the spectral domain of optical RS data, most TS pixels are a mixture of more than one temporal EM in the time domain. In the last decades, various algorithms have been proposed to accomplish the task of finding appropriate image derived EMs for SMA. Because the concept of convexity of geometry is natural and logical, N-finder (N-FINDR) (Winter 1999) is a popular and widely used technique for automatic EM identification. Therefore, this method is used to automatically extract temporal EMs in the present study. N-FINDR searches through a set of pixels with the largest possible volume by inflating a simplex. Mathematically expressed, the volume of a simplex spanned by a set of q temporal EM candidates $\mathbf{E} = \left[\boldsymbol{e}_1, \boldsymbol{e}_2, \ldots, \boldsymbol{e}_q\right]$ is proportional to the determinant of the set augmented by a row of ones. This is given by

$$V\left(\boldsymbol{e}_1, \boldsymbol{e}_2, \ldots, \boldsymbol{e}_q\right) = \frac{\left|\det\left(\begin{bmatrix} 1 & 1 & \ldots & 1 \\ \boldsymbol{e}_1 & \boldsymbol{e}_2 & \ldots & \boldsymbol{e}_q \end{bmatrix}\right)\right|}{(q-1)!} \tag{1}$$

For each pixel location in the input data, the volume is recalculated by testing the pixel at all q EM positions until no larger simplex volume is found. However, the determinant can only be defined when the number of features is $q-1$ due to matrix properties. We assume that the temporal vectors lie within or very close to a low-dimensional linear subspace, and the number of temporal EMs is typically much smaller than the number of temporal bands. In this study, the minimum noise fraction (Green et al. 1988), which ranks the obtained components according to their signal-to-noise ratios, is used to map high-temporal-dimensional data to a lower dimensional space.

Assuming the values for the individual pure EM component are linearly independent and the pixels in the TS image lie in linear spaces, linear unmixing is the simplest and the most practical approach to solve mixed pixel decomposition (Keshava and Mustard 2002). Let $\boldsymbol{r}_i$ be the i-th daily SIC trajectory of SIC TS $\mathbf{R}$. Each temporal pixel vector in the original image can be modelled using $\boldsymbol{r}_i = \sum_{j=1}^{q} a_{i,j}\boldsymbol{e}_j + \omega_i$, where $a_{i,j}$ denotes a FA of the temporal EM vector $\boldsymbol{e}_j$ at pixel $\boldsymbol{r}_i$ and ω_i is a noise vector. The least squares solution to computing FAs of $a_{i,j} = (\mathbf{E}^{\mathrm{T}}\mathbf{E})^{-1}\mathbf{E}^{\mathrm{T}}\boldsymbol{r}_i$ is derived by minimizing the pixel reconstruction error $\| \boldsymbol{r}_i - a_{i,j}\mathbf{E}\|^2$.

2.2. *TSA*

Over the last few decades, there is an increased interest in how we can predict future values from past observations. The time series model (TSM) is a powerful tool for developing an appropriate model that describes the inherent structures of data by examining past observations. The model is then used to predict future values of TS based on those of the past. Therefore, TS forecasting has been widely applied in numerous practical fields of study (Hipel and McLeod 1994). For successful TS forecasting, it is critical to develop an adequate model for underlying TS data. In recent years, numerous researchers have attempted to improve the accuracy of TS forecasting.

Those appealing features motivated the study of developing various types of TSMs, both at the theoretical level and in practical applications. Autoregressive (AR) models that relate current series values to past values and prediction errors were considered in this study on daily Antarctic SIC prediction using FAs derived from TMA as inputs of TSM. The AR model, which is a special case of the more general AutoRegressive Moving Average (ARMA) models that promise outcomes in forecasting environmental TS relative to competing models, specifies that the output variable depends linearly on its previous values and takes the form of a stochastic difference equation (Hipel and McLeod 1994; Piwowar and Ledrew 2010).

For example, if an AR model for an observation x_t at time t is expressed by a function ϕ of the previous value x_{t-1} plus white noise a_t, this relationship can be written as $x_t = \phi x_{t-1} + a_t$. This is the simplest AR model, referred to as AR(1). If we wish to predict the present value x_t using two previous measurements x_{t-1} and x_{t-2}, then the AR model would be as $x_t = \phi_1 x_{t-1} + \phi_2 x_{t-2} + a_t$. This model is a second-order autoregression, denoted AR(2). More generally, the AR model of order p can be defined as AR(p) and mathematically written as $x_t = \phi_1 x_{t-1} + \phi_2 x_{t-2} + \cdots + \phi_p x_{t-p} + a_t$, where $\phi_1, \phi_2, \ldots, \phi_p$ are parameters of the AR model. The AR model is simply a linear regression of the current value of the series against one or more prior values of the series. This is a multiple linear regression in which the value of the series at any time t is a linear function of values at times $t-1, t-2, \ldots, t-p$.

3. Experimental results

The experiments in this study were conducted in two stages: (1) TMA and (2) TSA. The first stage involved computing TS FAs of the representative temporal EMs for 36 years. In the second stage, the resulting FAs of the first stage were used to train TSMs and to predict new FAs. Each stage employed several parts, and more detailed information are provided in the following subsections.

3.1. *Stage 1: TMA*

The TMA stage to compute the corresponding FAs associated with the temporal EMs was identical to the experimental part of the previous study (Chi, Kim, and Kang 2016) and is comprised of three parts. First, we used the Harsanyi–Farrand–Chang virtual dimensionality algorithm (Harsanyi, Farrand, and Chang 1993) to determine the number of temporal EMs from 36 years of daily SIC data without prior knowledge. As there are numerous

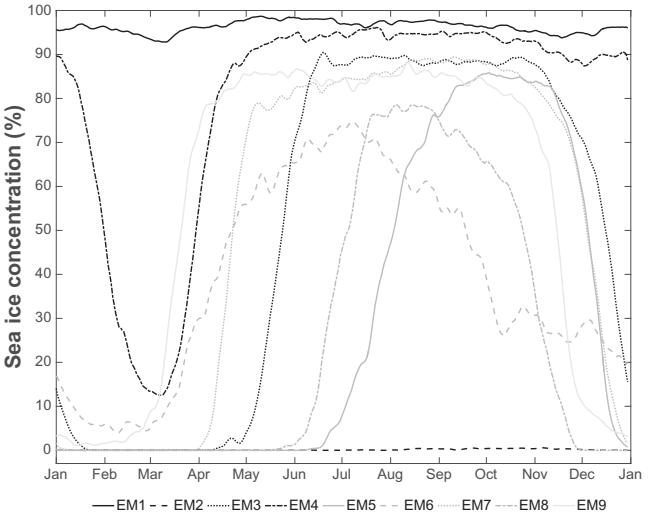

Figure 1. Temporal endmembers extracted using N-FINDR showing sea ice types (EM1: multi-year or fast ice; EM2: open sea; EM3-EM9: seasonal sea ice signatures).

anomalous SIC pixels in daily SIC data acquired from 1979 to 2013 due to sensor/processing errors or abnormal weather conditions, and data gaps from 1979 to 1987 due to acquisitions on alternating days, the data were reprocessed to generate consistent daily TS throughout the time period by smoothing method using neighbouring pixels and by gap-filling using linear interpolation, respectively. As a result, the number of potential temporal EMs was determined to be 9. Secondly, the N-FINDR algorithm was used to identify the representative temporal EMs showing the maximum variation in SIC throughout the year, as shown in Figure 1. Subsequently, the corresponding FAs associated with each temporal EM, which will be used as input variables for TSMs, were computed using a least square unmixing algorithm. For detailed information on this TMA stage and experimental results, refer to the paper by Chi, Kim, and Kang (2016).

3.2. *Stage 2: TSA*

3.2.1. *Single model determination*

The order of the models should be set for each TS to fit AR models appropriately to image data. Since our temporal image data acquired at a single temporal sequence include 82,907 valid pixels, 82,907 individual AR models are required to adequately apply all of the Antarctic SIC data. One of the objectives of this study was to automatically predict future SIC using TSA approaches. In practice, due to inefficiency of individually and manually fitting models to the 82,907 pixels, we assume that most of the Antarctic SIC for 36 years could be fitted with AR models of the same degree and that the single AR model is generally advisable for overall use.

To determine the order of the AR model for all of the SIC data, we first examined certain factors such as trends, seasonality and outliers. There may be notable seasonal trends in daily or monthly SIC, while there are no consistent trends or seasonality patterns and no obvious outliers appear over the entire period in terms of the FAs of

temporal EMs. The AR(1) is the simplest AR-type model for which we use a linear model to predict values for the present time by using the value of the previous time and thus may support our goal with respect to year-to-year forecasting.

The TSM of FAs of corresponding temporal EMs is produced by AR models and is inherently multivariate. One of the temporal EMs used to predict employs past and present values of every other temporal EM. For our data set, which includes 9 FA variables $[f_1, f_2, \ldots, f_9]$ with lag 1, the multivariate AR(1) model can be written as follows:

$$\begin{aligned} f_{1,t} &= \phi_{11,1} f_{1,t-1} + \phi_{12,1} f_{2,t-1} + \ldots + \phi_{19,1} f_{9,t-1} + a_{1,t} \\ f_{2,t} &= \phi_{21,1} f_{1,t-1} + \phi_{22,1} f_{2,t-1} + \ldots + \phi_{29,1} f_{9,t-1} + a_{2,t} \\ &\ldots \\ f_{9,t} &= \phi_{91,1} f_{1,t-1} + \phi_{92,1} f_{2,t-1} + \ldots + \phi_{99,1} f_{9,t-1} + a_{9,t} \end{aligned} \tag{2}$$

However, before the single AR model can be applied to all of the data sets, the AR(1) model must be statistically evaluated to determine whether all pixels accept the single AR(1) model. The accuracy of the AR model can be quantitatively determined based on the significance of the model parameter estimates. The significance, also referred to as the *t*-statistic, is determined by the ratio of each AR parameter estimate to its standard error (Piwowar and Ledrew 2010). A confidence interval gives an estimated range of values. All *t*-statistics greater than 2 are significant at the 95% confidence level. We applied the AR(1) model to all 82,907 valid FA TS for 35 years (1979–2013) and calculated *t*-statistics for each pixel location, and Figure 2 shows their spatial distribution. The white pixels are pixel locations that accepted the AR(1) model at a higher than 95% confidence level, and darker pixels are associated with lower confidence level regions that did not pass the test. As shown in Figure 2, the AR(1) model adequately fitted for most of the TS, indicating that the AR(1) model can be applied to all Antarctic regions as a single model assumption.

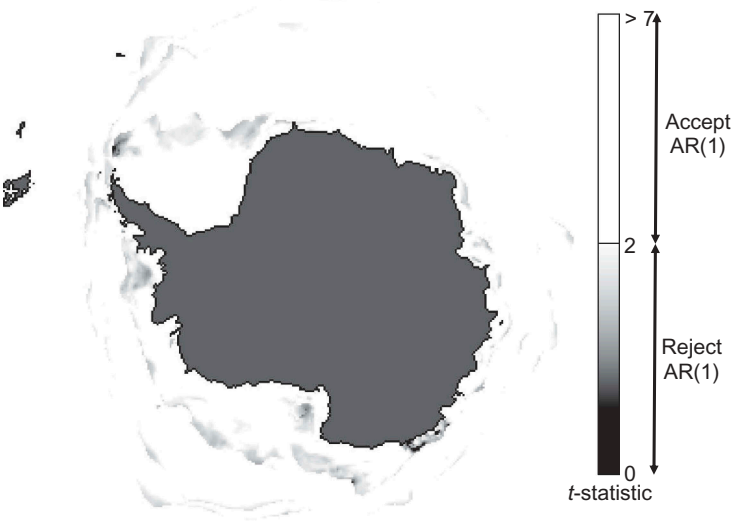

Figure 2. Spatial distribution of *t*-statistics.

3.2.2. *Experimental results*

Based on the assumption presented earlier, the entire TS of 35-year FAs for 1979–2013 derived by the TMA as inputs are used to train single AR(1) models, and to predict FAs for 2014. Combining resulting FAs associated with each temporal EMs and the representative temporal EM trajectories derived from the EM identification step of the TMA stage could reconstruct daily 365 SIC images for 2014 via the inverse process of spectral unmixing. To judge the quantitative accuracy of the predicted FAs for 2014 using the proposed method, the root-mean-square error (RMSE), which provides an overall 'pixel-by-pixel' difference between the original and reconstructed images, was advisable as it is straightforward to explain and does not show relative values.

Figure 3 illustrates the comparison of the original NSIDC SIC data (SIC_{NSIDC}) for the selected days (day of year (DOY): 30, 120, 210) in 2014 with two reconstruction SIC images using (1) FAs 'computed' via the spectral unmixing approach ($SIC_{compute}$)

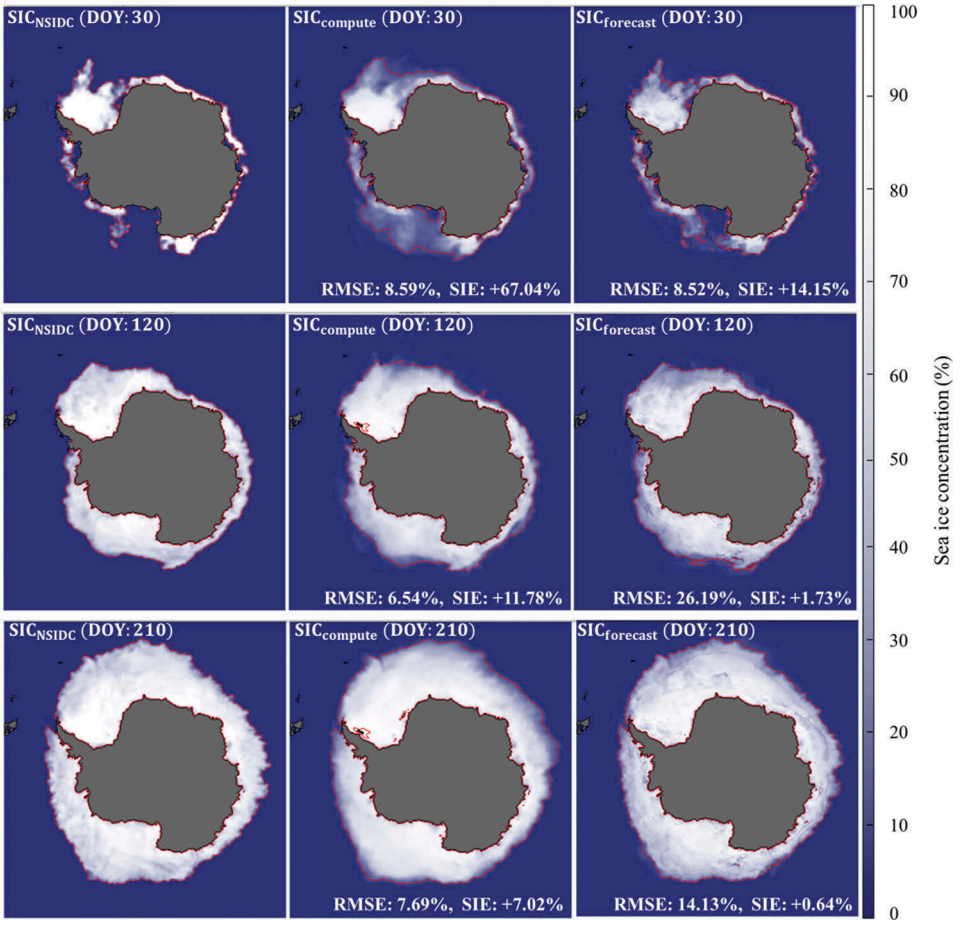

Figure 3. Daily SIC comparisons with errors. The figures in different columns show SIC patterns on DOY of 30, 120 and 210, and the figures in different rows show SIC patterns obtained from the original NSDIC (left), computed via the pixel unmixing approach proposed in Chi, Kim, and Kang (2016) (middle), and predicted via the single AR model proposed in this study (right).

proposed in Chi, Kim, and Kang (2016) and (2) FAs 'predicted' via the single AR(1) model ($SIC_{forecast}$) proposed in the present study. Red borders in each image denote sea ice extents (SIEs), where the regions of interest present SIC values of at least 15%. The both reconstructed SIC images ($SIC_{compute}$, $SIC_{forecast}$) did not generally capture detailed SIC variability in local regions and resulted in smoother SIC estimates than the original data as discussed in Chi, Kim, and Kang (2016). As shown in Figure 3, however, both concentrations and extents typically exhibited good visual agreement with the original images. As a quantitative validation, RMSE values between SIC_{NSIDC} and $SIC_{compute}$ had a range of 4.42–11.76% and the mean accuracy was 8.46% with corresponding standard deviation 1.54%. For comparisons with $SIC_{forecast}$, RMSE ranged from 7.25% to 26.64% and its mean was 12.89% with standard deviation of 4.68%. Overall, the results indicate that $SIC_{compute}$ are statistically reconstructed better than $SIC_{forecast}$. $SIC_{forecast}$ visually appears to capture better local variability than $SIC_{compute}$ in some regions, but produces relatively low statistical fidelity with SIC_{NSIDC} for some areas. These regions may be associated with the AR(1) model rejected areas and it results in low statistical accuracy. For interpreting the SIEs shown in Figure 3, the proposed prediction method showed better visual agreement and statistical accuracy. Overall extents (red borders) generated by predicted FAs ($SIE_{forecast}$) exhibited higher visual agreement with the original extents (SIE_{NSDIC}) than those produced by real FAs ($SIE_{compute}$). Besides, daily averages of summed areas for all grid cells in $SIE_{forecast}$ estimated approximately 2.5% more SIEs (standard deviation: 3.46%), while $SIE_{compute}$ was overestimated by approximately 15% with larger standard deviation. Therefore, it should be noted that the proposed forecasting method helped to reconstruct SICs and to define SIEs compared to reconstruction images using computed fractions.

Figure 4 illustrates the original SIC trajectories ($SICT_{NSIDC}$, solid line), reconstructed SIC trajectories based on computed FAs of the previous study (Chi, Kim, and Kang 2016)

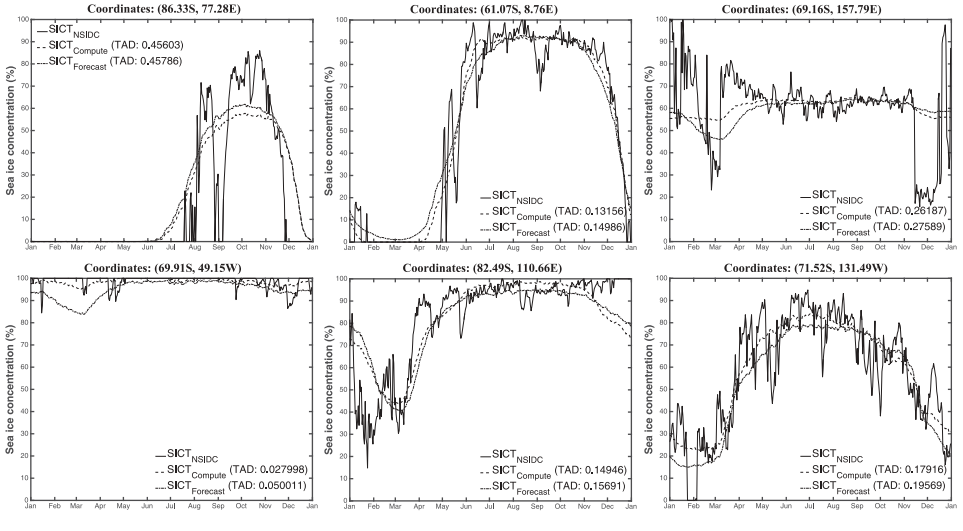

Figure 4. Comparisons of the original, computed, and forecasted SIC trajectories at the selected locations.

($SICT_{compute}$, dashed line), and reconstructed SIC trajectories at the selected locations based on forecasted FAs used in this study ($SICT_{forecast}$, dash-dot line). The DOY and SIC are plotted on the *x*-axis and *y*-axis, respectively. As shown in Figure 4, $SICT_{NSIDC}$ presents very noisy curves, potentially due to the presence of processing errors in SIC retrieval algorithms, sensor errors or meteorological conditions. Overall, however, both $SICT_{compute}$ and $SICT_{forecast}$ generally showed similar shapes as those of $SICT_{NSIDC}$, and they minimized and mitigated noise effects, as they were reconstructed using representative temporal EMs. As discussed in the previous study (Chi, Kim, and Kang 2016), the reconstructed images did not frequently contain or minimize the impacts of anomalies. As shown in Figure 4, both $SICT_{compute}$ and $SICT_{forecast}$ in the selected regions were visually similar, but the temporal angle distance (TAD), which is mathematically identical to spectral angle distance, between the $SICT_{NSIDC}$ and $SICT_{compute}$ was slightly better than the TADs between the $SICT_{NSIDC}$ and $SICT_{forecast}$. Overall, the average pixel-per-pixel TADs are 0.4007 and 0.4458 for $SICT_{compute}$ and $SICT_{forecast}$ of the valid 82,907 pixels, respectively. As discussed in these experimental results, the single AR(1) model generally fitted to our SIC data and adequately forecasted FAs, and our proposed method thus effectively forecasted SICs.

4. Conclusions

In this study, FAs for the past 35 years computed using the TMA approach were incorporated with AR(1) models in an effort to forecast new FAs for the present year. The proposed approach was fully data-driven without considering physical processes. The forecasted FAs were used to compute reconstructed images using representative temporal EMs identified through TMA. Several contributions of this study can be summarized as follows. First, as most TS of FA values of Antarctic SICs could be fitted to AR(1) models, the single model proved to be appropriate for overall use. Second, although the proposed method did not produce quantitatively accurate total amount of SIC compared to the spectral unmixing approach proposed in Chi, Kim, and Kang (2016), it is better to reproduce total area of SIC. The proposed results were found to be comparable with real values in terms of overall RMSE, visual agreement, and TAD. The proposed method might be more useful to create SIE maps than SIC calculation. Third, both reconstructed SICTs resulted in smoother curves than the original trajectories as the representative temporal EMs extracted from 35-year SIC data did not frequently include anomalies.

Furthermore, the findings and our assessment of the current work may lead to the following extensions. First, although most TS were fitted to the single AR(1) model, approximately 10% of the pixel locations within the total pixels did not accept the AR (1) model. As there may be appropriate AR models for these rejected TS, we will develop an adaptive model selection algorithm to find the best fit. Second, the most critical aspect of TMA relates to the identification of temporal EMs. As TS forecasting based on TMA results uses FAs computed from temporal EMs and the linear mixture model, improvements to the EM selection algorithm, such as by exploiting spatial context, which is a distinguishing characteristic of image data, are worth further study.

Disclosure statement

No potential conflict of interest was reported by the authors.

Funding

This work was supported by the Korea Polar Research Institute [PE16040].

References

Cavalieri, D. J., Parkinson, C. L., P. Gloersen, and H. J. Zwally. 1996. "Sea Ice Concentrations from Nimbus-7 SSMR and DMSP SSM/I-SSMIS Passive Microwave Data, Natl." *Snow and Ice Data Cent., Boulder, Colo.[Updated yearly.]*. doi:10.5067/8GQ8LZQVL0VL.

Chi, J., H.-C. Kim, and S.-H. Kang. 2016. "Machine Learning-Based Temporal Mixture Analysis of Hypertemporal Antarctic Sea Ice Data." *Remote Sensing Letters* 7 (2): 190–199. doi:10.1080/2150704X.2015.1121300.

Comiso, J. C., D. J. Cavalieri, C. L. Parkinson, and P. Gloersen. 1997. "Passive Microwave Algorithms for Sea Ice Concentration: A Comparison of Two Techniques." *Remote Sensing of Environment* 60 (3): 357–384. doi:10.1016/S0034-4257(96)00220-9.

Green, A. A., M. Berman, P. Switzer, and M. D. Craig. 1988. "A Transformation for Ordering Multispectral Data in Terms of Image Quality with Implications for Noise Removal." *IEEE Transactions on Geoscience and Remote Sensing* 26 (1): 65–74. doi:10.1109/36.3001.

Harsanyi, J. C., W. H. Farrand, and C.-I. Chang. 1993. "Determining the Number and Identity of Spectral Endmembers: An Integrated Approach Using Neyman-Pearson Eigen-Thresholding and Iterative Constrained RMS Error Minimization." *The Thematic Conference on Geologic Remote Sensing*, San Antonio, TX, February, 395.

Hipel, K. W., and A. I. McLeod. 1994. *Time Series Modelling of Water Resources and Environmental Systems*, Amsterdam: Elsevier, 63–86.

Ivanova, N., O. M. Johannessen, L. T. Pedersen, and R. T. Tonboe. 2014. "Retrieval of Arctic Sea Ice Parameters by Satellite Passive Microwave Sensors: A Comparison of Eleven Sea Ice Concentration Algorithms." *IEEE Transactions on Geoscience and Remote Sensing* 52 (11): 7233–7246. doi:10.1109/TGRS.2014.2310136.

Keshava, N., and J. F. Mustard. 2002. "Spectral Unmixing." *IEEE Signal Processing Magazine* 19 (1): 44–57. doi:10.1109/79.974727.

Li, W., and C. Wu. 2014. "Phenology-Based Temporal Mixture Analysis for Estimating Large-Scale Impervious Surface Distributions." *International Journal of Remote Sensing* 35 (2): 779–795. doi:10.1080/01431161.2013.873147.

Li, W., and C. Wu. 2015. "Incorporating Land Use Land Cover Probability Information into Endmember Class Selections for Temporal Mixture Analysis." *ISPRS Journal of Photogrammetry and Remote Sensing* 101: 163–173. doi:10.1016/j.isprsjprs.2014.12.007.

Piwowar, J. M., and E. F. Ledrew. 2010. "ARMA Time Series Modelling of Remote Sensing Imagery: A New Approach for Climate Change Studies." *International Journal of Remote Sensing* 23 (24): 5225–5248. doi:10.1080/01431160110109552.

Piwowar, J. M., D. R. Peddle, and E. F. Ledrew. 1998. "Temporal Mixture Analysis of Arctic Sea Ice Imagery: A New Approach for Monitoring Environmental Change." *Remote Sensing of Environment* 63 (3): 195–207. doi:10.1016/S0034-4257(97)00105-3.

Screen, J. A. 2011. "Sudden Increase in Antarctic Sea Ice: Fact or Artifact?" *Geophysical Research Letters* 38: 13. doi:10.1029/2011GL047553.

Winter, M. E. 1999. "N-FINDR: An Algorithm for Fast Autonomous Spectral End-Member Determination in Hyperspectral Data." *SPIEs International Symposium on Optical Science, Engineering, and Instrumentation*, Denver, CO, July 18, 266–275.